Available online at www.sciencedirect.com

jmr&t Journal of Materials Research and Technology

journal homepage: www.elsevier.com/locate/jmrt

Original Article

Investigation of hard-burn and soft-burn lime kiln dust as alternative materials for alkali-activated binder cured at ambient temperature

Peerapong Jitsangiam [a], *Teewara Suwan* [a,*], *Pitiwat Wattanachai* [b], *Weerachart Tangchirapat* [c], *Prinya Chindaprasirt* [d], *Mizi Fan* [e]

[a] *Center of Excellence in Natural Disaster Management, Department of Civil Engineering, Faculty of Engineering, Chiang Mai University, Chiang Mai, 50200, Thailand*

[b] *Department of Civil Engineering, Faculty of Engineering, Chiang Mai University, Chiang Mai, 50200, Thailand*

[c] *Department of Civil Engineering, Faculty of Engineering, King Mongkut's University of Technology Thonburi, Bangkok, 10140, Thailand*

[d] *Sustainable Infrastructure Research and Development Center, Department of Civil Engineering, Faculty of Engineering, Khon Kaen University, Khon Kaen, 40002, Thailand*

[e] *Department of Civil Engineering, College of Engineering, Design and Physical Sciences, Brunel University, Uxbridge, UB8 3PH, London, United Kingdom*

ARTICLE INFO

Article history:
Received 31 August 2020
Accepted 24 October 2020
Available online 2 November 2020

Keywords:
Alkali-activated binder
Ambient curing temperature
Lime kiln dust
Hard-burn LKD
Soft-burn LKD

ABSTRACT

As climate change becomes a severe concern, the development of green technology becomes a goal for many sectors, including the construction material sector. Ordinary Portland cement (OPC), the main constituent of concrete production, is a primary contributor to releasing carbon dioxide (CO_2) into the atmosphere. Some alternative cementitious materials have been studied to reduce the massive amount of OPC consumption. Lime kiln dust (LKD), a by-product of quicklime production, is produced in abundance worldwide and mostly disposed of in landfills. The two types of LKD, soft-burn and hard-burn, are high-potential wastes that can be developed as alternative cementitious binders using the alkali-activated binder (AAB) technology. This study investigates the mixture designation and properties of LKD-based AAB when cured at ambient temperature. The results show that an ambient-cured soft-burn LKD-AAB achieved practical workability with an 8 M NaOH solution, 1.50 of sodium silicate-to-sodium hydroxide ratio (SS/SH), and 0.60 of liquid alkaline-to-binder ratio (L/B). A rapid setting behavior and an excellent compressive strength of 10.89 MPa at 28 days were revealed at room temperature curing. The ambient-cured hard-burn LKD-AAB could not provide the appropriate properties. However, the mixture of 20% hard-burn LKD and 80% soft-burn LKD resulted in an LKD-AAB mixture that meets the minimum requirement for low-strength cement applications. The positive outcome of this study may be the solution for of LKD wastes utilization in Thailand that addresses the challenge of developing ambient-cured AAB for in-field applications.

* *Corresponding author.*
E-mail address: teewara.s@cmu.ac.th (T. Suwan).

https://doi.org/10.1016/j.jmrt.2020.10.069

1. Introduction

Ordinary Portland cement (OPC) is one of the most widely used construction materials in the world. OPC production is projected to increase from roughly 2.5 billion tons in 2006 to 5 billion tons in 2050. Portland cement is a gray powder produced mainly from calcination of limestone ($CaCO_3$) to yield calcium oxide (CaO) as a final product. Although there are many advantages of using OPC, a major drawback is the massive amount of carbon dioxide (CO_2) emissions during its burning process. It is reported that one ton of OPC production releases approximately 0.90 tons of CO_2 to the atmosphere [1]. Various alternative materials have been introduced to replace OPC as an approach to more sustainable green construction. These materials include fly ash, calcined clay, calcium carbide residue, blast furnace slag, construction and demolition material, crushed-rock, and lime kiln dust [2–10].

Limestone is also a primary raw material of quicklime (CaO) production, similar to OPC. Burning limestone at 800 to 1000 °C results in quicklime with gases and fine dust particles, which are captured by a filter collector in an air pollution control system (e.g., cyclones, baghouses, and electrostatic precipitators), producing lime kiln dust (LKD) as a by-product [11]. There are two types of LKD, soft-burn and hard-burn LKD. Soft-burn LKD has a soft-white color and is initially collected by an attached filter. Soft-burn LKD can be re-calcined in a kiln to produce more quicklime. This second cycle in the kiln yields a by-product called hard-burn LKD. Quicklime is used in many industries, e.g., steel purification, chemical reagent production, food and agricultural production, mining, construction, and wastewater treatment [12]. Thus, a massive amount of LKD is produced but is mostly disposed of into landfills globally [13]. The US generates approximately 2.5–3.6 million tons of LKD annually [9,14]. Furthermore, around 10,000 to 20,000 tons of LKD are collected by Thailand's manufacturers each year [15].

Many studies have been performed on LKDs as a replacement material for OPC. Arulrajah [8] investigated the strength and durability of recycled construction and demolition wastes stabilized with LKD. Other studies have indicated that OPC can be partially replaced with approximately 20% LKD and 10% fly ash and used as cementitious binders to achieve optimum properties for infrastructure applications [8,16,17]. LKD was also used to expedite construction on wet clay soils as modified pavement subgrades [18]. In addition, reconstituted samples using 4%–8% LKD with fly ash added by static compaction have shown to provide effective stabilization for weak soil [19,20]. LKD has been investigated to replace OPC directly. In one study, an increase of LKD in the concrete mix reduced the over-compressive strength of hardened concrete, concluding that LKD can replace up to 60% of OPC for some low-strength applications [21].

Another approach was to apply LKD in an alternative green cementitious material called alkali-activated binder (AAB), also known as Geopolymer cement [22]. AAB is a cementitious binder that uses alkaline activators (e.g., soluble silicate and soluble hydroxide) to activate aluminosilicate raw materials. Fresh AAB is typically cured in a heating chamber for 6–48 h at 40–90 °C to accelerate the reaction [22]. AAB is then cured at ambient temperature for further handling and installation. The mechanical properties of the AAB, according to relevant standards used for OPC, are equivalent or superior to those of OPC [23,24]. The main advantage of AAB technology is that any by-products containing silica (SiO_2), alumina (Al_2O_3), and calcium (Ca) can be used as a raw material [25]. Heat curing is vital in increasing the strength of an AAB. However, high calcium content can cause materials to set rapidly and harden prematurely [23]. With the careful design of mixtures and well-prepared production, sufficient mechanical properties can be achieved in ambient curing conditions [26].

This research investigates the properties of AAB using LKD as raw material cured at ambient temperature. The novelty of this study can be highlighted in two approaches. The first is developing 100% LKD as a primary raw material through AAB technology. The second is incorporating impracticable hard-burn LKD in conjunction with high potential soft-burn LKD (soft-to-hard–burn LKD proportion). Consequently, both soft- and hard-burn LKDs are investigated as alternative binders for producing a low-strength AAB material for the construction industry.

2. Materials

2.1. Lime kiln dust

Two types of LKD, soft- and hard-burn, were collected from Chememan Public Company Limited, Saraburi Province, Thailand. Soft-burn LKD has a soft white color, while hard-burn LKD is dark gray. Fig. 1a and b shows pictures and grain size distributions of soft- and hard-burn LKDs, respectively. The median grain size d_{50} of soft-burn LKD is 0.13 mm and of hard-burn LKD is 0.12 mm. The two types of LKD were graded by sieving through an ASTM standard mesh no. 200 (i.e., <75 μm) before using them as cementitious binders. Their chemical compositions, identified by energy dispersive X-ray fluorescence (EDXRF), are shown in Table 1. Both types of LKD contained a high percentage of CaO, as limestone ($CaCO_3$) is the parent material. The small amounts of Al_2O_3, SiO_2, Fe_2O_3, etc. were also detected as constituents and impurities in the mineral.

Loss on ignition (LOI) from the typical ranges of LKD resulted in an average LOI value (soft-burn LKD) of roughly 22.9%–29.1%, while the high LOI value (hard-burn LKD) was approximately 36.4% [26,27]. Higher LOI values of hard-burn LKD indicate a higher carbon content, porosity, and water absorption than soft-burn LKD [28,29].

2.2. Alkaline activators

Sodium hydroxide (NaOH, SH) and sodium silicate (Na_2SiO_3, SS) were used as alkaline activators for the LKD-based AAB synthesis. A laboratory-grade micro-pearl sodium hydroxide with 99% purity was purchased from ACI Labscan Ltd., Thailand. The NaOH solid was dissolved in distilled water to form a NaOH solution in a specific concentration in molarity (M). Sodium silicate solution (SL-2.4C) was purchased from Union Science Co., Ltd., Thailand, with sodium silicate of

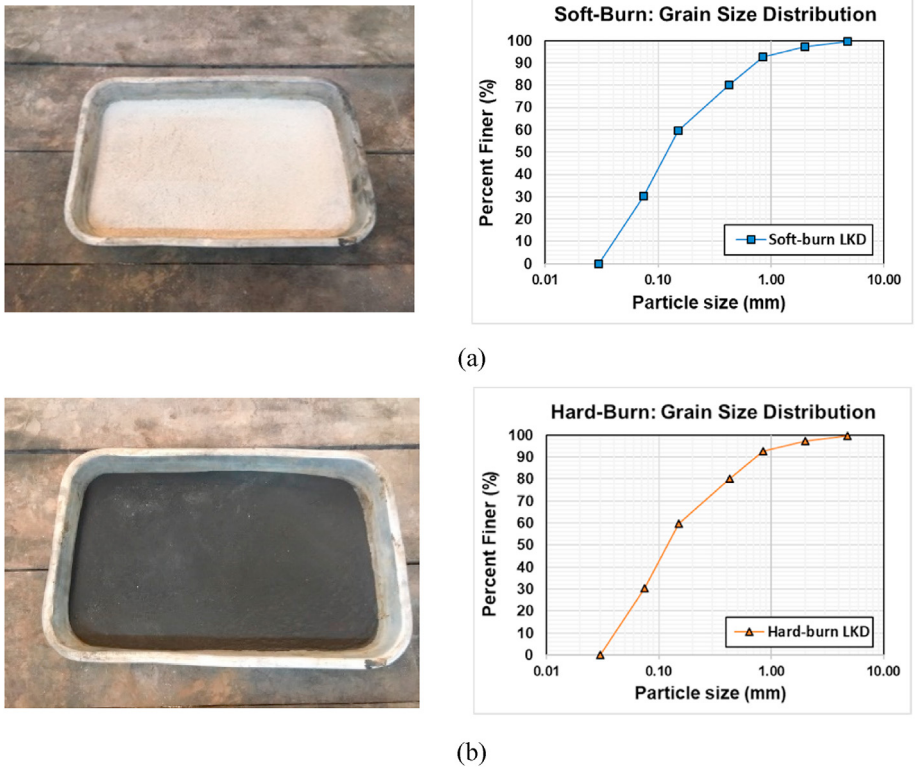

Fig. 1 – Soft-burn (a) and hard-burn (b) LKD and their grain size distribution.

45.83% w/w. The soluble silicate modulus M_s was 2.41, with 13.44% Na_2O and 32.39% SiO_2.

3. Mixture designation and testing methodology

The investigation of the AAB synthesis using LKD as a raw material was divided into two groups based on vital factors. An analysis of all the test results determined minimal-cost approaches of LKD utilization as a cementitious binder.

3.1. *Mixture designation and sample preparation*

3.1.1. *Hard- and soft-burn LKD for AAB paste synthesis cured at ambient temperature*

Early strength development of every LKD-based AAB synthesized from hard- and soft-burn is required. The feasibility of each LKD operating as a cementitious material was first evaluated. The mixtures comprised 10 M NaOH solution and a constant ratio of the liquid alkaline activator to binder (L/B) of 0.60. The ratio of sodium silicate solution to NaOH solution (SS/SH) was gradually increased (0.67, 1.00, and 1.50). The water-to-solid ratio (w/s) is defined as the total mass of water used in the NaOH solution and sodium silicate solution to the total mass of all solids from LKD, micro-pearl NaOH, and sodium silicate solid. The strength development and the effects of alkaline dosage on a soft-burn LKD-AAB paste were also studied as follows:

Part 1. With variable SS/SH, the NaOH activator concentration was varied from 8 M to 10 M–12 M. A constant L/B of 0.60 maintained preferable workability. SS/SH values were gradually increased through five levels (0.67, 1.00, 1.50, 2.00, and 2.50). Table 2 shows the mix proportions and water-to-solid ratios of the soft-burn LKD-AAB paste in various NaOH Concentrations and SS/SH values.

Part 2. With variable L/B, the concentration of NaOH was 8 M. The SS/SH was set to 1.50. The L/B was gradually increased through six levels (0.40, 0.50, 0.55, 0.60, 0.65, and 0.70) and tested at each level. Table 3 shows the mix of the proportions and water-to-solid ratios of the soft-burn LKD-AAB paste at various L/B values.

3.1.2. *Proportions of soft-to sard-burn LKD-based AAB paste cured at ambient temperature*

The strength development of combined soft-to hard-burn LKD was investigated to utilize the inert hard-burn LKD as a replacement for AAB. A concentration of NaOH activator of 8 M was used. The L/B was 0.60, and the SS/SH was 1.50. Table 4 shows the mix proportions of soft- and hard-burn LKDs. Seven mixtures were prepared by increasing the Hard-burn LKD replacement percentage. The overall w/s ratio of all mixtures was equal to 0.308.

Table 1 – Chemical composition of soft- and hard-burn LKD by EDXRF.

Oxide	Al_2O_3	SiO_2	CaO	SO_3	K_2O	Fe_2O_3	TiO_2
Soft-burn LKD	1.45	4.60	90.73	0.57	–	2.64	–
Hard-burn LKD	1.23	3.96	88.77	2.12	1.19	2.37	0.37

Table 2 – Mixtures of hard-burn and soft-burn LKD-AAB paste in various NaOH concentrations and SS/SH ratios.

Mixture	NaOH (M)	L/B	SS/SH	LKD (g)	NaOH Sol. (g)	Na_2SiO_3 Sol. (g)	w/s
H10M_0.67	10	0.60	0.67	1500.0	538.9	361.1	0.319
H10M_1.00			1.00	1500.0	450.0	450.0	0.308
H10M_1.50			1.50	1500.0	360.0	540.0	0.297
S8M_0.67	8	0.60	0.67	1500.0	538.9	361.1	0.336
S8M_1.00			1.00	1500.0	450.0	450.0	0.322
S8M_1.50			1.50	1500.0	360.0	540.0	0.308
S8M_2.00			2.00	1500.0	300.0	600.0	0.299
S8M_2.50			2.50	1500.0	257.1	642.9	0.292
S10M_0.67	10	0.60	0.67	1500.0	538.9	361.1	0.319
S10M_1.00			1.00	1500.0	450.0	450.0	0.308
S10M_1.50			1.50	1500.0	360.0	540.0	0.297
S10M_2.00			2.00	1500.0	300.0	600.0	0.290
S10M_2.50			2.50	1500.0	257.1	642.9	0.285
S12M_0.67	12	0.60	0.67	1500.0	538.9	361.1	0.304
S12M_1.00			1.00	1500.0	450.0	450.0	0.296
S12M_1.50			1.50	1500.0	360.0	540.0	0.287
S12M_2.00			2.00	1500.0	300.0	600.0	0.282
S12M_2.50			2.50	1500.0	257.1	642.9	0.278

Note. The mixture name specifies the concentrations. For example, H10M_0.67 represents hard-burn LKD (H) with ten molar NaOH concentration (10 M) and an SS/SH of 0.67, while S8M_0.67 represents soft-burn LKD (S) with eight molar NaOH concentration (8 M) and an SS/SH of 0.67.

Table 3 – Mixtures of soft-burn LKD AAB paste at various L/B ratios.

Mixture	NaOH (M)	SS/SH	L/B	LKD (g)	NaOH Sol. (g)	Na_2SiO_3 Sol. (g)	w/s
S_L/B0.40	8	1.50	0.40	1500.0	240.0	360.0	0.219
S_L/B0.50			0.50	1500.0	300.0	450.0	0.265
S_L/B0.55			0.55	1500.0	330.0	495.0	0.287
S_L/B0.60			0.60	1500.0	360.0	540.0	0.308
S_L/B0.65			0.65	1500.0	390.0	585.0	0.329
S_L/B0.70			0.70	1500.0	420.0	630.0	0.349

Note. The mixture name S_L/B0.40 represents soft-burn LKD with an L/B of 0.40, for example.

For all mixtures, the mixing processes started with the preparation of alkaline solutions. NaOH and sodium silicate solutions were first mixed together to form a homogeneous solution. LKDs and the prepared alkaline solutions were then added in a standard Hobart mixer. After thoroughly mixing for 2 min, the mixer was stopped for 30 s to move all adhered pastes to the middle of the mixing pot. The mixer was restarted and ran for another 2 min. The freshly blended LKD-based AAB paste was cast into prepared 4 × 4 × 16 cm molds (BS EN 196-1). A vibration table with a 2-min period was used for compaction. Next, all specimens were immediately wrapped in plastic film and kept at room temperature (26 ± 3 °C) for 24 h. They were then removed from the molds and kept at room temperature until they reached the age needed for testing.

3.2. *Analytical techniques*

Setting times for the LKD-based AAB were determined by using a Vicat needle apparatus with ASTM C191-a18 [30],

Table 4 – Mixtures between soft- and hard-burn types of LKD-based AAB.

Mixtures	LKD (%)		LKD (g)		NaOH (M)	L/B	SS/SH
	Soft	Hard	Soft	Hard			
S100_H0	100	0	1500.0	0.0	8	0.60	1.50
S80_H20	80	20	1200.0	300.0	8	0.60	1.50
S60_H40	60	40	900.0	600.0	8	0.60	1.50
S50_H50	50	50	750.0	750.0	8	0.60	1.50
S40_H60	40	60	600.0	900.0	8	0.60	1.50
S20_H80	20	80	300.0	1200.0	8	0.60	1.50
S0_H100	0	100	0.0	1500.0	8	0.60	1.50

Note. The mixture name S80_H20 means 80% soft-burn LKD and 20% hard-burn LKD by weight were used.

and the flow tests were carried out in accordance with ASTM C1437-15 [31]. The compressive strength tests were performed on a 250 kN Control universal testing machine (UTM) with the British standard EN 196-1 [32]. The samples were tested at the age of three days and 28 days. A four-circle kappa goniometer X-Ray diffraction (XRD) machine with microfocus sealed tube (Mo) and direct photon counting detector (HyPixBantam) was used to analyze the structural formation of the resulting products along with the Cambridge Structure Database (CSD). The oxide molar ratios were calculated to observe the relationships among the reactions and chemical compositions of the AAB.

4. Results and discussion

4.1. *Characteristics and early strength development of AAB paste using hard-burn and soft-burn LKD*

Each hard- and soft-burn LKD-AAB mixture, identified in Section 3.1.1, was visually inspected to determine its individual characteristics, including early strength development at three days age (Fig. 2). Although the LKDs with specific alkaline dosages were easily cast into the molds with sufficient workability, the Hard-burn AAB paste reached a high viscosity with the prolonged setting. Early strength development of both doft- and hard-burn LKDs was investigated (Table 5).

The early strength of both soft- and hard-burn AAB pastes increased as SS/SH increases, from 3.56 to 10.10 MPa for the soft-burn type and 0.55–0.79 MPa for the hard-burn type. The higher SS/SH provided more silica into the system and enhanced the binders' reactions. Moreover, the soft-burn LKD achieved a higher strength than the hard-burn LKD. Although their chemical compositions were similar, using a double-burning process could have led to a high carbon (C) content in hard-burn LKD (analyzed by EDXRF and LOI values). The carbon not only made the paste dark gray but also retarded the reaction, leading to a prolonged setting time with low compression capability.

Table 5 – Compressive strength of LKD-based AAB Pastes at three days age.

LKD type	NaOH (M)	L/B	SS/SH	Compressive strength (MPa)
Soft-burn	10	0.60	0.67	3.56
			1.00	5.82
			1.50	10.10
Hard-burn	10	0.60	0.67	0.55
			1.00	0.83
			1.50	0.79

The main finding of this investigation of the properties of Soft-burn and Hard-burn types of LKD is that Soft-burn LKD has more potential to be developed as a cementitious binder because of its workability and the strength it gains. Therefore, the next experiments were carried out with Soft-burn LKD, as seen in the next section.

4.2. *Influence of the dosage of an alkaline activator on strength development and oxide molar ratio*

The influence of alkaline dosages on the strength development of soft-burn LKD-based AAB paste cured at ambient temperature was investigated. The average compressive strengths at different NaOH concentrations and SS/SH values are presented in Fig. 3. At each SS/SH, the soft-burn LKD-AAB noticeably strengthened as the concentration of NaOH increased from 8 to 12 M.

Strong alkalinity from the NaOH solution provided higher dissolution rates for the major compositions in LKD, namely, calcium, silicon, and aluminum. This leads to more significant polymerization for the formation. The highest overall strength was achieved in a mixture with an SS/SH of 2.00 and 12 M NaOH at 11.77 MPa. The SS/SH ratio in AAB synthesis refers to the amount of sodium silicate solution, which manifests as an

Fig. 2 – AAB Paste Produced from soft-burn LKD (left) and hard-burn LKD (right).

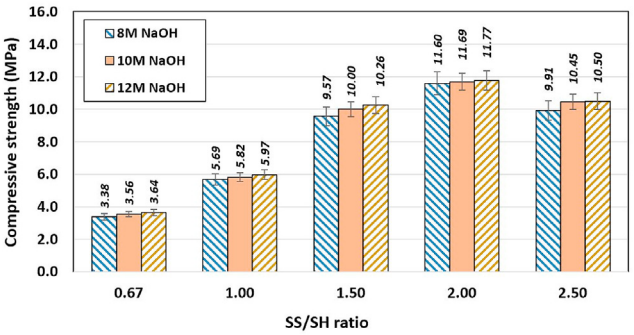

Fig. 3 – Compressive strength of soft-burn LKD-based AAB in various alkaline dosages at 28 days age.

additional source of silica in the cement mixture. As soluble silicate generally increases binding activity after the dissolution process, an increase in sodium silicate (i.e., an increase in overall silica content) could lead to a more complete polymerization and thorough bonding. However, a coagulated formation may develop, leading to an incomplete structure if excessive soluble silicate is applied. The compressive strength, therefore, dropped slightly at a higher SS/SH of 2.50 with 12 M NaOH (10.50 MPa).

As the result was mainly influenced by chemical reactions, the oxide molar values of the AAB mixtures were calculated based on the mass of the constituents and oxide molecular weights [26]. The amount of consumed LKD, NaOH, and Na_2SiO_3 solutions were taken into account to calculate the oxide molar values when the L/B was set to 0.60. Oxide molar values of all 15 mixtures are presented in Table 6. With a specified amount of LKD as the parent material, the oxide molars of CaO and Al_2O_3 were constant at 2426.80 and 21.33, respectively. Increasing the SS/SH from 0.67 to 2.50 increased the amount of SiO_2 and Na_2O in the system, while the amount of H_2O was significantly reduced. Therefore, the overall w/s decreased, leading to a low flowability of the prepared mixtures. The NaOH activator is commonly split into Na_2O and H_2O of oxide forms. The oxide molar of Na_2O rose when the concentration of NaOH increased from 8 to 12 M. Since the higher NaOH concentration contained more NaOH solid, the w/s values in the system were thus decreased. For example, the w/s of the S8M_0.67 mixture was reduced from 0.336 to 0.319 in the S10M_0.67 mixture and 0.304 in the S12M_0.67 mixture.

In AAB chemistry, the oxide molar ratio is widely used to identify the final properties of cementitious products. Examples of ratios that are analyzed include SiO_2/Al_2O_3, CaO/SiO_2, Na_2O/Al_2O_3, and H_2O/Na_2O. The oxide molar ratios of soft-burn LKD-AAB at NaOH concentrations of 8, 10, and 12 M are shown in Fig. 4.

In general, the SiO_2/Al_2O_3 value in a formation would be roughly 1 to 5, which shows the capability of their cross-link extension to the ring chain of polymer (Si–O–Al). A structure model is found mainly to be amorphous to semi-crystalline phases [33]. This ratio in the soft-burn-based AAB increased as SS/SH rose from 0.67 to 2.50. However, the SiO_2/Al_2O_3 range of 14–22 in the experiment indicates the formation of a high crystalline structure of C–S–H (calcium silicate hydrate) and C-A-S-H (calcium alumino-silicate hydrate) from the high amount of CaO content in LKD [34].

The CaO/SiO_2 indicates the proportion of calcium to silica in the system. Previous research has found that a fast setting occurs in mixtures with a CaO/SiO_2 higher than 3. However, in this test, CaO/SiO_2 values of approximately 5–8 were observed and decreased when the SS/SH increased. Higher CaO/SiO_2 allows for faster setting as well as early strength development because of the formation of the C–S–H and C-A-S-H phases [20,35,36].

Na_2O/Al_2O_3 indicates the level of alkalinity and the amount of reactive Al_2O_3 in an AAB system. The presence of Na^+ has a role in balancing charges with Al^-in the structure. Generally, the mixture with Na_2O/Al_2O_3 values between 0.6 and 15 can harden and gain strength. The test of soft-burn LKD-AAB resulted in Na_2O/Al_2O_3 of 10–14, indicating an ability to form and gain strength in ambient curing conditions. In addition, Na_2O/Al_2O_3 values decreased slightly with higher SS/SH values.

The H_2O/Na_2O value is the amount of water to sodium oxide from the alkaline activators. In general, a cement sample cannot set if H_2O/Na_2O is higher than 25. However, with an H_2O/Na_2O value around 11 to 14, all mixtures of soft-burn

Table 6 – Oxide molar of mixture in soft-burn LKD AAB pastes.

Mixtures	L/B	CaO	SiO_2	Al_2O_3	Na_2O	H_2O	w/s
S8M_0.67	0.60	2426.80	309.46	21.33	241.63	3518.24	0.336
S8M_1.00		2426.80	357.39	21.33	233.96	3384.63	0.322
S8M_1.50		2426.80	405.90	21.33	226.20	3249.41	0.308
S8M_2.00		2426.80	438.24	21.33	221.03	3159.26	0.299
S8M_2.50		2426.80	461.34	21.33	217.33	3094.86	0.292
S10M_0.67	0.60	2426.80	309.46	21.33	270.81	3417.77	0.319
S10M_1.00		2426.80	357.39	21.33	258.33	3300.75	0.308
S10M_1.50		2426.80	405.90	21.33	245.69	3182.30	0.297
S10M_2.00		2426.80	438.24	21.33	237.27	3103.33	0.290
S10M_2.50		2426.80	461.35	21.33	231.25	3046.92	0.285
S12M_0.67	0.60	2426.80	309.46	21.33	296.82	3328.22	0.304
S12M_1.00		2426.80	357.39	21.33	280.04	3225.96	0.296
S12M_1.50		2426.80	405.90	21.33	263.07	3122.47	0.287
S12M_2.00		2426.80	438.24	21.33	251.75	3053.48	0.282
S12M_2.50		2426.80	461.35	21.33	243.66	3004.19	0.278

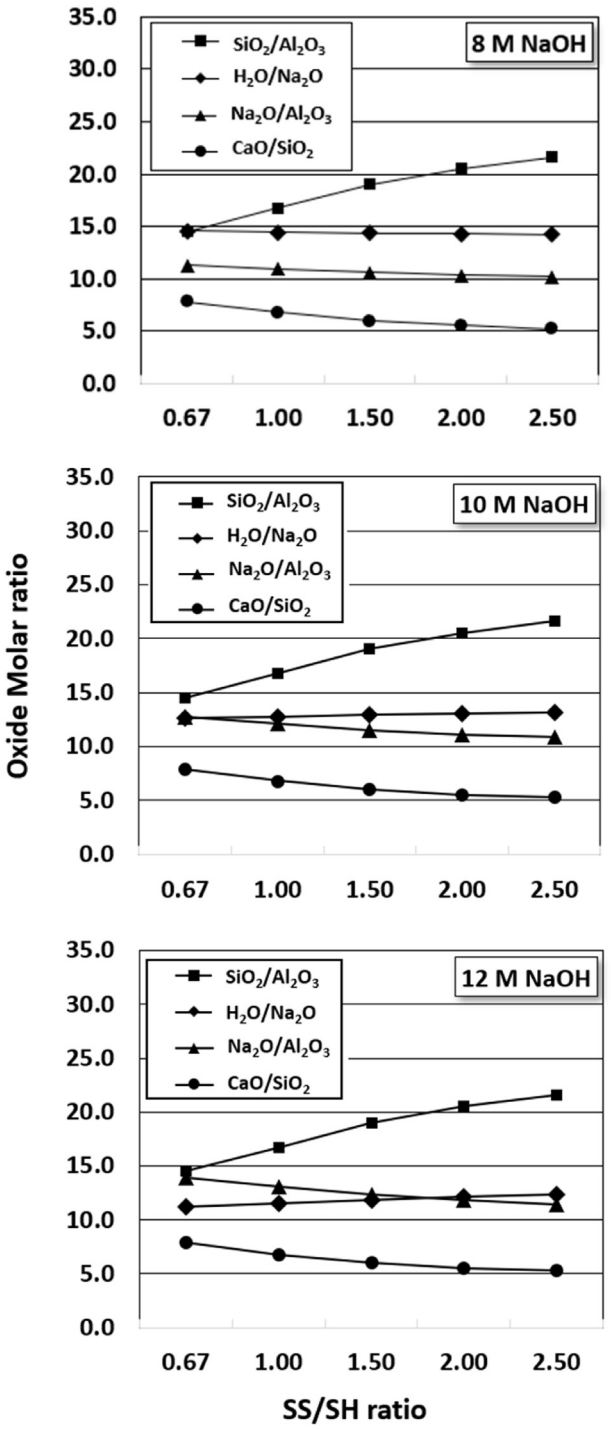

Fig. 4 – Oxide molar ratios of soft-burn LKD-AAB at NaOH concentrations of 8 (top), 10 (middle), and 12 M (bottom).

LKD-AAB hardened adequately. It is noted that the H_2O/Na_2O value decreases when the SS/SH rises from 0.67 to 2.50 in a low NaOH concentration (8 M), but it increases in the higher NaOH concentrations of 10 and 12 M [34,37,38].

In summary, soft-burn LKD mixed with an 8 M NaOH solution and an SS/SH of 1.50 achieves the highest strength. This option is also the most cost-effective use of alkaline activators owing to the least amount of costly NaOH used. Workability and setting time, the critical factors for practical work, are tested on various L/B values in the next section.

4.3. *Influence of liquid-to-binder ratios on workability and strength development*

In addition to the optimal dosage of applied alkaline activators, the influence of L/B was investigated. L/B in AAB synthesis is partially comparable to the water-to-cement (w/c) ratio in Portland cement production, as both indicate the amount of water in the system. However, the amount of water in liquid alkaline (L) must be recalculated from the concentrated solution before comparing it to water (w) in the Portland cement mixture. The 8 M NaOH solution and an SS/SH of 1.50 were used in this experiment. Six L/B values (0.40, 0.50, 0.55, 0.60, 0.65, and 0.70) were analyzed to investigate the workability, setting behavior, and strength in ambient curing conditions for in-field operation of the soft-burn LKD-AAB.

Setting time and flowability of selected mixtures of the soft-burn LKD-AAB were observed in various L/B values (see Table 7). The setting time for OPC paste is typically around 30 min and 10 h for initial and final settings, respectively. As LKD obtains high calcium content, the formation of an AAB structure is mainly dominated by C–S–H, C-A-S-H, and some phases of sodium alumino-silicate hydrate (N-A-S-H). The presence of those formations led to a range of 2–9 min for the initial setting time and 6–20 min for the final setting time for this experiment. The setting times lengthened when the L/B increased, similar to an increase of in w/s. This may contribute to the early strength approach for some specific purposes, such as repairing cement. A low L/B of 0.40 stiffens the mixture limiting its ability to perform a flow test, while a high L/B makes the mixture too watery. The results show that an appropriate L/B is between 0.50 and 0.60 to maintain flowability at 100–140%.

As L/B values directly affect both overall water content and the amount of alkaline activator, an increase in strength was, therefore, clearly evident, as shown in Fig. 5. The compressive strengths of all mixtures were developed by the times from three to 28 days. Gaps in strength between the two ages were not significant, as early strength was already obtained on the first day, and all the mixtures were cured at ambient temperature. The w/s values increased along with L/B. However, the highest strength was achieved by the soft-burn LKD-AAB

Table 7 – Setting time and flowability of soft-burn LKD-AAB with various L/B values.

Mixtures	L/B	Setting time (min)		Flow (%)
		Initial	Final	
S_L/B0.40	0.40	2.5	6.0	–[a]
S_L/B0.50	0.50	3.5	10.0	99.31
S_L/B0.55	0.55	5.5	12.0	140.73
S_L/B0.60	0.60	7.5	15.0	141.74
S_L/B0.65	0.65	8.5	18.0	–[b]
S_L/B0.70	0.70	9.5	20.0	–[b]

[a] Flash setting.
[b] Too watery to measure the flow.

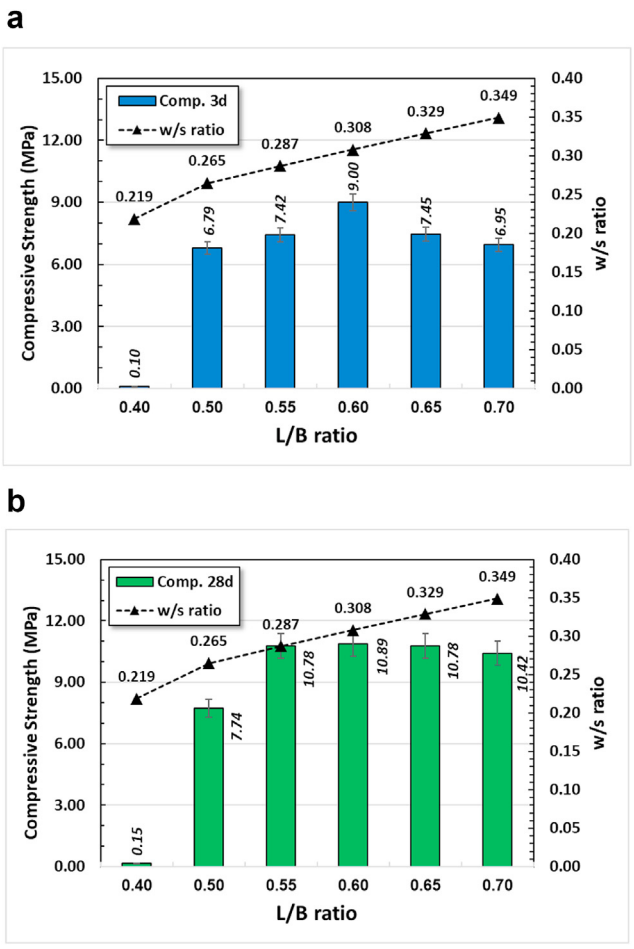

Fig. 5 – Compressive strength and w/s ratio of Soft-burn LKD AAB in various L/B ratios. Fig. 5a. Compressive strength and w/s at three days. Fig. 5b. Compressive strength and w/s at 28 days.

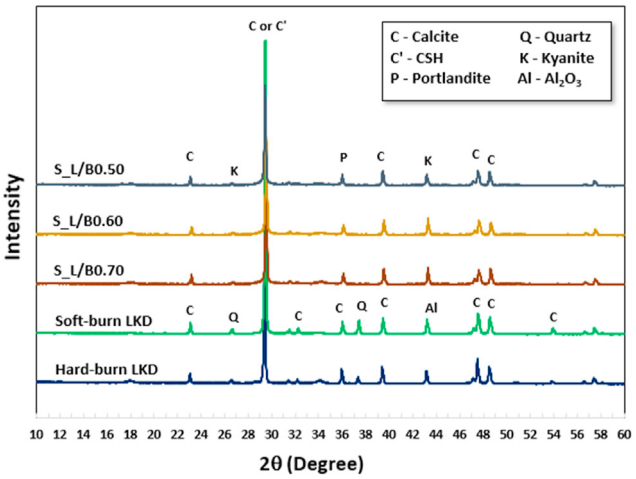

Fig. 6 – X-ray diffraction patterns of LKD powders and soft-burn LKD-AAB mixtures.

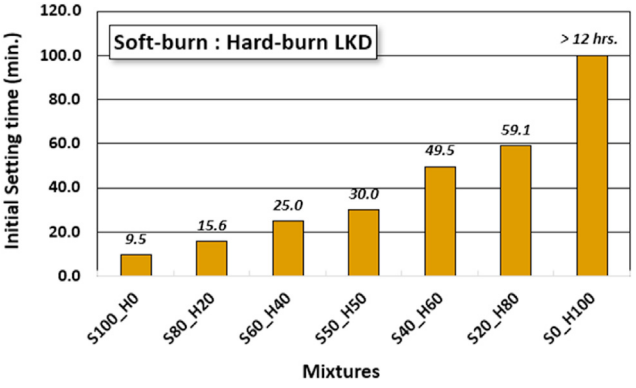

Fig. 7 – Initial setting time of soft- and hard-burn LKD blended AAB mixtures.

when the L/B was 0.60, reaching 9.0 MPa and 10.89 MPa at three days and 28 days, respectively.

In Fig. 6, XRD patterns of original soft- and hard-burn LKD materials reveal the structure formation of calcite in $CaCO_3$ form, referring to the depleting amount of calcium content. Quartz and aluminum oxide refer to crystalline SiO_2 and Al_2O_3 in LKD materials, respectively. Similar XRD results, as well as EDXRF of soft- and hard-burn LKD, are presented. There were significant differences in the high carbon content of the hard-burn LKD compared to that soft-burn LKD.

Three mixtures of soft-burn LKD-AAB with an L/B of 0.50, 0.60, and 0.70 were compared to the original LKD powder. Quartz and aluminum compound (Al) in original LKD at 2θ values of 26.6°, 37.3°, and 43.2° were transformed to Kyanite (K), an alumino-silicate compound (Al_2O_5Si) in the structure. Portlandite (P) or $Ca(OH)_2$ also were found at $2\theta = 36.1°$ (S_L/B0.50, S_L/B0.60, S_L/B0.70) after polymerization as calcite was merged with OH^- from the alkaline activator. Calcium silicate hydrate (C'; C–S–H) and calcium alumino-silicate hydrated (C-A-S-H) were the polymerization products from the massive amount of calcite presented at $2\theta = 28.4°$. From the XRD database, the chemical formula of C–S–H is $Ca_5Si_6O_{16}(OH)_2 \cdot 4H_2O$ or Tobermorite, while C-A-S-H is $CaAl_2Si_2O_8 \cdot 4(H_2O)$. A broad hump indicating a polymerized amorphous phase was not observed. The strength was mainly governed by the mostly crystalline structure, which

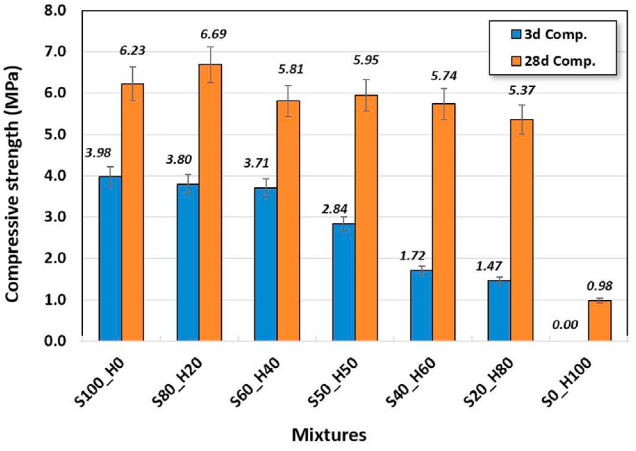

Fig. 8 – Compressive strength of soft- and hard-burn LKD-AAB mixtures.

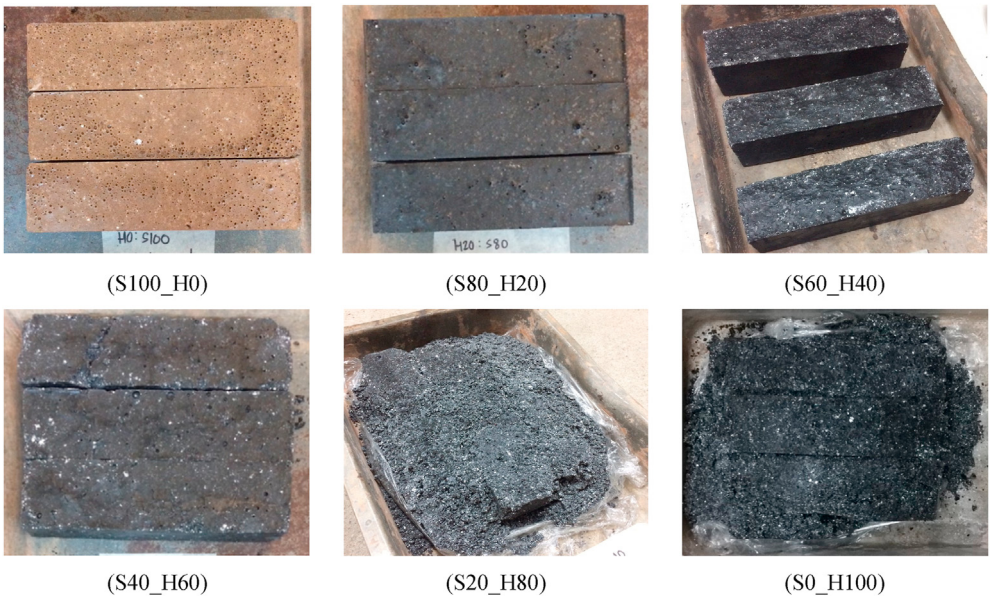

Fig. 9 – Appearance of specimens in various soft- and hard-burn ratios.

appeared to shape peak patterns. The final products may, therefore, be classified as semi-crystalline phases or AAB.

The findings of this section determine the appropriate L/B for AAB production. An L/B ratio of 0.60 provided a suitable setting time and excellent flowability for AABs with high calcium content, as well as maximum strength at both three days and 28 days of age.

4.4. *Combinations of soft-burn and hard-burn LKD for possible AAB production*

The amount of hard-burn LKD replacement in soft-burn LKD-based AAB was studied. This section aims to apply the main findings of the previous sections in AAB constituents and to utilize the massive amount of hard-burn LKD wastes. Soft-burn LKD was replaced by hard-burn LKD at 20%, 40%, 50%, 60%, 80%, and 100%. An 8 M NaOH solution with SS/SH of 1.50 and an L/B of 0.60 were selected for these mixtures of soft- and sard-burn LKD-AABs. Initial setting time and compressive strength were determined to verify the potentiality of such blends in practical production.

The 100% soft-burn LKD-AAB (S100_H0) provided a rapid initial setting time of fewer than 10 min, as shown in Fig. 7. However, the initial setting time increased as more hard-burn LKD was used. The 100% hard-burn LKD-AAB (S0_H100) did not set within the first 12 h of casting into the mold (Fig. 7).

Similar to the test results in section 4.1, the compressive strength of soft- and hard-burn LKD-AAB mixtures aged three days and aged 28 days were serially decreased when the amount of hard-burn replacement increased. A hard-burn replacement of 20% (S80_H20) achieved the highest strength (6.69 MPa) at 28 days, while the lowest strength capability was the pure hard-burn LKD type (S0_H100), only 0.98 MPa at 28 days (Fig. 8).

Fig. 9 shows the six samples after the 28 days. The color of the samples becomes darker as the amount of hard-burn LKD increases. Consistent with the strength gained, firm and compact specimens were observed in the mixture with low hard-burn content, e.g., S80_H20 and S60_H40. On the contrary, the samples with high hard-burn replacement (S20_H80 and S0_H100) were crumbly.

5. Conclusions

This paper investigated the properties and feasibility of using hard- and soft-burn LKD as an alternative starting material for AAB cement synthesis cured at ambient temperature. Concluding remarks are as follows:

- Soft-burn LKD achieved higher compressive strength than hard-burn LKD. The double-burning process for hard-burn LKD created a high amount of carbon, causing the dark gray color, retarding the reaction, prolonging the setting time, and yielding low strength capability.
- Soft-burn AAB synthesis at ambient temperature with 8 M NaOH solution, an SS/SH of 1.50, and an L/B of 0.60 provided a suitable setting time, excellent flowability, and optimal strength. This mixture provided appropriate AAB constituents for practical work processes of in-field applications with the most cost-effective use of alkaline activators.
- Mixtures of soft- and hard-burn LKD in the proper proportions can yield acceptable mechanical properties for low-strength applications. The addition of hard-burn LKD extended the mixture setting times and allowed more time for the practical operation, although the strength significantly decreased. A hard-burn replacement of 20% (S80_H20) achieved the highest strength (6.69 MPa) at 28

days. With the introduced constituents, both soft- and hard-burn LKD can be used as an alternative for producing a low-strength cementitious material for the construction industry.

6. Recommendations for future research

This primary study aimed to investigate the potential combinations of soft- and hard-burn LKDs and their mechanical properties for AAB production. At this stage, both studied LKDs proved to have the potential for use in synthesizing the AAB through the strength and XRD observations. However, for future research, the formation of internal compounds in the AAB, likely using the Fourier-transform infrared spectroscopy (FTIR) technique and determination of the morphology of the AAB using the scanning electron microscope (SEM) technique, should be performed.

Author contributions

Peerapong Jitsangiam: Conceptualization, Methodology, Writing-Review & Editing, Visualization, Investigation, Formal analysis.

Teewara Suwan: Conceptualization, Methodology, Writing-Original Draft, Writing-Review & Editing, Visualization, Investigation, Formal analysis.

Pitiwat Wattanachai: Writing-Review & Editing, Visualization, Investigation, Formal analysis.

Weerachart Tangchirapat: Writing-Review & Editing, Visualization, Investigation, Formal analysis.

Prinya Chindaprasirt: Writing - Review & Editing, Supervision, Formal analysis

Mizi Fan: Writing-Review & Editing, Supervision, Formal analysis

Declaration of Competing Interest

The authors declare that they have no known competing financial interests or personal relationships that could have appeared to influence the work reported in this paper.

Acknowledgments

All authors would like to express gratitude to the Department of Civil Engineering, Faculty of Engineering, Chiang Mai University (CMU) for the use of its equipment and facilities. Also, this research work was partially supported by Chiang Mai University. The fifth author would like to acknowledge the financial support of the Thailand Research Fund (TRF) under the TRF Distinguished Research Professor Grant No. DPG6180002. Furthermore, the authors would like to acknowledge the financial support and the raw materials for these experiments from Chememan Public Company Limited, Thailand.

REFERENCES

[1] Hasanbeigi A, Price L, Lin E. Emerging energy-efficiency and CO2 emission-reduction technologies for cement and concrete production: a technical review. Renew Sustain Energy Rev 2012;16(8):6220–38.
[2] Andini S, Cioffi R, Colangelo F, Grieco T, Montagnaro F, Santoro L. Coal fly ash as raw material for the manufacture of geopolymer-based products. Waste Manag 2008;28(2):416–23.
[3] Fernandez R, Martirena F, Scrivener KL. The origin of the pozzolanic activity of calcined clay minerals: a comparison between kaolinite, illite and montmorillonite. Cement Concr Res 2011;41(1):113–22.
[4] Phetchuay C, Horpibulsuk S, Suksiripattanapong C, Chinkulkijniwat A, Arulrajah A, Disfani MM. Calcium carbide residue: alkaline activator for clay-fly ash geopolymer. Construct Build Mater 2014;69:285–94.
[5] Huseien GF, Sam ARM, Shah KW, Asaad MA, Tahir MM, Mirza J. Properties of ceramic tile waste-based alkali-activated mortars incorporating GBFS and fly ash. Construct Build Mater 2019;214:355–68.
[6] Silva RV, De Brito J, Dhir RK. Properties and composition of recycled aggregates from construction and demolition waste suitable for concrete production. Construct Build Mater 2014;65:201–17.
[7] Jitsangiam P, Suwan T, Pimraksa K, Sukontasukkul P, Chindaprasirt P. Challenge of adopting relatively low strength and self-cured geopolymer for road construction application: a review and primary laboratory study. Int J Pavement Eng 2019:1–15.
[8] Arulrajah A, Mohammadinia A, D'Amico A, Horpibulsuk S. Effect of lime kiln dust as an alternative binder in the stabilization of construction and demolition materials. Construct Build Mater 2017;152:999–1007.
[9] Rashad AM. A brief on high-volume Class F fly ash as cement replacement–A guide for Civil Engineer. Int J Sustain Bulit Environ 2015;4(2):278–306.
[10] Rashad AM. An overview on rheology, mechanical properties and durability of high-volume slag used as a cement replacement in paste, mortar and concrete. Construct Build Mater 2018;187:89–117.
[11] Miller MM, Callaghan RM. Lime kiln dust as a potential raw material in Portland cement manufacturing. Open-File Report 2004–1336. US Geological Survey; 2004 [Online Only].
[12] Latifi N, Rashid ASA, Marto A, Tahir MM. Effect of magnesium chloride solution on the physico-chemical characteristics of tropical peat. Environ Earth Sci 2016;75(3):220.
[13] Issa MA. Efficient and beneficial use of industrial by-products in concrete technology. In: Geo-frontiers 2011: advances in geotechnical engineering; 2011. p. 1182–91.
[14] Apodaca Lori E. Lime. Geological Survey ed. Mineral commodity summaries 2020. Government Printing Office; 2020.
[15] Chememan. Lime production process. 2019. http://www.chememan.com/en/product-services/all-about-lime/lime-production-process.
[16] Kadhim A, Sadique M, Al-Mufti R, Hashim K. Long-term performance of novel high-calcium one-part alkali-activated cement developed from thermally activated lime kiln dust. J Bulid Eng 2020;32:101766.
[17] Mohammadinia A, Arulrajah A, D'Amico A, Horpibulsuk S. Alkali activation of lime kiln dust and fly ash blends for the stabilisation of demolition wastes. Road Mater Pavement Des 2020;21(6):1514–28.

[18] Bandara N, Hettiarachchi H, Jensen E, Binoy TH. Upcycling potential of industrial waste in soil stabilization: use of kiln dust and fly ash to improve weak pavement subgrades encountered in Michigan, USA. Sustainability 2020;12(17):7226.
[19] Chen R, Drnevich VP, Daita RK. Short-term electrical conductivity and strength development of lime kiln dust modified soils. J Geotech Geoenviron Eng 2009;135(4):590–4.
[20] Kang X, Ge L, Kang GC, Mathews C. Laboratory investigation of the strength, stiffness, and thermal conductivity of fly ash and lime kiln dust stabilised clay subgrade materials. Road Mater Pavement Des 2015;16(4):928–45.
[21] Latif MA, Naganathan S, Razak HA, Mustapha KN. Performance of lime kiln dust as cementitious material. Procedia Eng 2015;125:780–7.
[22] Davidovits J. Geopolymers: inorganic polymeric new materials. J Therm Anal Calorim 1991;37(8):1633–56.
[23] Suwan T, Fan M. Influence of OPC replacement and manufacturing procedures on the properties of self-cured geopolymer. Construct Build Mater 2014;73:551–61.
[24] Chindaprasirt P, Chareerat T, Sirivivatnanon V. Workability and strength of coarse high calcium fly ash geopolymer. Cement Concr Compos 2007;29(3):224–9.
[25] Suwan T. Categories and types of raw materials using in geopolymer cement production: an overview. In: Solid state phenomena, vol. 280. Trans Tech Publications Ltd; 2018. p. 481–6.
[26] Temuujin JV, Van Riessen A, Williams R. Influence of calcium compounds on the mechanical properties of fly ash geopolymer pastes. J Hazard Mater 2009;167(1–3):82–8.
[27] Wattanachai P, Suwan T. Strength of geopolymer cement curing at ambient temperature by non-oven curing approaches: an overview. In: IOP conference series: materials science and engineering, vol. 212. IOP Publishing; 2017, June. p. 12–4. 1.
[28] Button JW. Kiln dust for stabilization of pavement base and subgrade materials. , Texas, USA: Texas Transportation Institute College Station; 2003.
[29] Xiao X, Yang H, Zhang H, Lu J, Yue G. Research on carbon content in fly ash from circulating fluidized bed boilers. Energy Fuel 2005;19(4):1520–5.
[30] ASTM C191-a18. Standard test methods for time of setting of hydraulic cement by Vicat needle. ASTM International; 2019.
[31] ASTM C1437-15. Standard test method for flow of hydraulic cement mortar. ASTM International; 2015.
[32] BS EN 196-1. Methods of testing cement–Part 1: determination of strength. 2019.
[33] Hardjito D, Wallah SE, Sumajouw DM, Rangan BV. Factors influencing the compressive strength of fly ash-based geopolymer concrete. Civil Eng Dimens 2004;6(2):88–93.
[34] Davidovits J. Years of successes and failures in geopolymer applications. Market trends and potential breakthroughs. In: Geopolymer 2002 conference, vol. 28. Geopolymer Institute; 2002, October. p. 29.
[35] Suwan T, Fan M, Braimah N. Internal heat liberation and strength development of self-cured geopolymers in ambient curing conditions. Construct Build Mater 2016;114:297–306.
[36] Pimraksa K, Chindaprasirt P, Setthaya N. Synthesis of zeolite phases from combustion by-products. Waste Manag Res 2010;28(12):1122–32.
[37] Pimraksa K, Chindaprasirt P, Huanjit T, Tang C, Sato T. Cement mortars hybridized with zeolite and zeolite-like materials made of lignite bottom ash for heavy metal encapsulation. J Clean Prod 2013;41:31–41.
[38] Wan Q, Rao F, Song S, García RE, Estrella RM, Patino CL, et al. Geopolymerization reaction, microstructure and simulation of metakaolin-based geopolymers at extended Si/Al ratios. Cement Concr Compos 2017;79:45–52.